Study of the Rate Type Fluid with Temperature Dependent Viscosity

Naeem Faraz[a] and Yasir Khan[b]

[a] Modern Textile Institute, Donghua University, 1882 Yan'an Xilu Road, Shanghai 200051, China

[b] Department of Mathematics, Zhejiang University, Hangzhou 310027, China

Reprint requests to N. F. and Y. K.; E-mail: nfaraz_math@yahoo.com and yasirmath@yahoo.com

Z. Naturforsch. **67a,** 460 – 468 (2012) / DOI: 10.5560/ZNA.2012-0050
Received January 4, 2012 / revised April 26, 2012

This paper outlines a comprehensive study of the two dimensional flow of an incompressible viscoelastic fluid over a shrinking/stretching sheet with temperature dependent viscosity. The governing coupled nonlinear differential equations are solved by means of the homotopy analysis method (HAM). The results are presented graphically to interpret various physical parameters appearing in the problem. The solution procedure explicitly elucidates the remarkable accuracy of the proposed algorithm.

Key words: Homotopy Analysis Method; Variable Viscosity.

1. Introduction

Abundance of literature deals with the flows of viscous fluids by employing Navier–Stokes equations [1 – 6]. But there are many fluids with complex microstructure that cannot be described by these equations. These fluids which exhibit a nonlinear relationship between the stresses and the rate of strain are called non-Newtonian fluids. They are increasingly being recognized as more appropriate in modern technological applications in comparison with Newtonian fluids. The constitutive equations of these fluids lead to flow problems in which the order of the differential equations exceeds the number of available conditions. The solutions of resulting problems for non-Newtonian fluids are in general more difficult to obtain. This is not only true for exact analytic solutions but even for numerical solutions.

In recent years, the rate type fluid models have received special attention. The first viscoelastic rate type model, which is still used widely, is due to Maxwell. Maxwell himself recognized that some liquids have a trend for storing energy and a means for dissipating energy, the storing of energy characterizing the fluid's elastic response and the dissipation of energy characterizing its viscous nature. The Maxwell model [7 – 12] is the simplest subclass of rate type fluids which takes into consideration the stress relaxation effects. Extensive analytical and numerical studies have been undertaken which involve such fluids. Important studies to the topic include the works in [7 – 15].

Flow of a fluid is also of great importance, and flow inside the thin film is another rich area which has attracted the attention of many researchers. This is due to their several applications in engineering such as wire and fiber coating reactor fluidization, polymer processing, foodstuff processing, transpiration cooling, and gaseous diffusion. In open literature, there are different methods by which one can tackle the nonlinear problems related to fluid phenomena such as the variational iteration method [16], the homotopy perturbation transform method [17], the trigonometric function series method [18], the mapping method [19], the modified trigonometric function series method [20], the bifurcation method [21], the $\left(\frac{G'}{G}\right)$-expansion method [22], dynamical systems approach [23], and the homotopy analysis method [24 – 26].

Thin film flow due to stretching or shrinking phenomena has been discussed by a number of workers such as Wang and Pop [27], Liu and Anderson [28], Dandapat et. al [29], Nadeem and Awais [30], Nadeem and Faraz [31], Raftari et al. [32], Yıldırım and Sezer [33], and Khan et al. [34, 35]. Nadeem and Awais [30] discussed the thin film flow of an unsteady shrinking sheet through the porous medium with variable viscosity and further extended this analysis for a second-grade fluid [31]. The aim of the present at-

tempt is to venture further in this regime [30, 31] for a rate type fluid. Also the main motivation is to work out analytical solutions for the steady thin film flow of a rate type fluid over a shrinking/stretching sheet with variable viscosity together with heat transfer analysis via homotopy analysis method. The developed analytical solution by the homotopy analysis method is sketched and discussed.

2. Problem Formulation

Consider an incompressible two-dimensional Maxwell fluid lying in a thin liquid film of uniform thickness $h(x)$ on a horizontal elastic sheet which converges to a narrow slot at the origin of a Cartesian coordinate system, see Figure 1. The fluid motion within the film arises due to stretching/shrinking of a porous elastic sheet. The flow and heat transfer characteristics are governed by the following equations. The x-axis is taken along the surface, and the y-axis is normal to it. The velocity and temperature fields in the thin liquid films are governed by the following boundary layer equations:

$$\frac{\partial u}{\partial x}+\frac{\partial v}{\partial y}=0, \tag{1}$$

$$u\frac{\partial u}{\partial x}+v\frac{\partial u}{\partial y}+\lambda_1\left(u^2\frac{\partial^2 u}{\partial x^2}+v^2\frac{\partial^2 u}{\partial y^2}+2uv\frac{\partial^2 u}{\partial x\partial y}\right) =\frac{1}{\rho_0}\frac{\partial}{\partial y}\left(\mu\frac{\partial u}{\partial y}\right), \tag{2}$$

$$u\frac{\partial T}{\partial x}+v\frac{\partial T}{\partial y}=\frac{1}{\rho_0 C_\mathrm{p}}\frac{\partial}{\partial y}\left(k\frac{\partial T}{\partial y}\right), \tag{3}$$

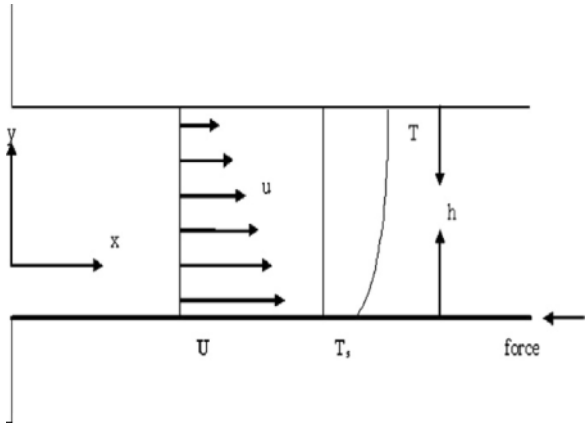

Fig. 1. Schematic diagram of thin film flow problem.

where u and v are the velocity components along x- and y-axis, respectively, T is the temperature, ρ_0 the density, μ the viscosity, k the thermal conductivity, and C_p the specific heat. The associated boundary conditions for the thin flow are

$$u=U(x),\ v=-V_0,\ T=T_\mathrm{s}\ \text{at}\ y=0, \tag{4}$$

$$\left[1+\lambda_1\left(u\frac{\partial}{\partial x}+v\frac{\partial}{\partial y}-\frac{\partial u}{\partial x}-\frac{\partial v}{\partial y}\right)\right]S_{xy} =\mu\frac{\partial u}{\partial y},\ \frac{\partial T}{\partial y}=0,\ v=u\frac{\mathrm{d}h}{\mathrm{d}x}\ \text{at}\ y=h. \tag{5}$$

In the above equations, $U(x)=bx$ is the stretching velocity $(b>0)$ corresponding to stretching and $(b<0)$ corresponding to the shrinking, λ_1 is the relaxation time, T_s the surface temperature, V_0 the suction velocity, and h the thickness of the film. We introduce the nondimensional variables $f(\eta)$ and $\theta(\eta)$ as well as similarity variables like η and variation of the viscosity and thermal conductivity with temperature etc.:

$$\eta=\left(\frac{b}{\nu_0}\right)^{1/2}y, \tag{6}$$

$$T=T_0+T_\mathrm{ref}\left[\frac{bx^2}{2\nu_0}\right]\theta(\eta), \tag{7}$$

$$\mu=\mu_0\exp[-\zeta(T-T_0)], \tag{8}$$

$$k=k_0[1+C(T-T_0)], \tag{9}$$

$$T_\mathrm{s}=T_0+T_\mathrm{ref}\left[\frac{bx^2}{2\nu_0}\right], \tag{10}$$

where T_0 and T_ref are the constant temperatures, k_0 is the constant of the thermal conductivity, and ν_0 is the constant viscosity, $C>0$ for fluids such as water and air, while $C<0$ for fluids such as lubrication oils. ψ is the stream function which automatically assures mass conservation in (1). The velocity components in terms of the stream function can be written as

$$u=\frac{\partial\psi}{\partial y}=bx\frac{\partial f(\eta)}{\partial\eta}, \tag{11}$$

$$v=-\frac{\partial\psi}{\partial x}=-(b\nu_0)^{1/2}f(\eta). \tag{12}$$

Making use of (11) and (12), (2) and (3) yield

$$f\frac{\partial^2 f}{\partial\eta^2}-\left(\frac{\partial f}{\partial\eta}\right)^2-\lambda\left(f^2\frac{\partial^3 f}{\partial\eta^3}-2f\frac{\partial f}{\partial\eta}\frac{\partial^2 f}{\partial\eta^2}\right) =(1-A\theta)\left[A\frac{\partial\theta}{\partial\eta}\frac{\partial^2 f}{\partial\eta^2}-\frac{\partial^3 f}{\partial\eta^3}\right], \tag{13}$$

$$\Pr\left[2\frac{\partial f}{\partial \eta}\theta - f\frac{\partial \theta}{\partial \eta}\right] = (1-\delta\theta)\frac{\partial^2\theta}{\partial\eta^2} - \delta\left(\frac{\partial\theta}{\partial\eta}\right)^2, \tag{14}$$

where

$$\delta = -C[T_s - T_0],\ A = -\zeta(T_s - T_0),\ S = \left(\frac{bv_0}{V_0^2}\right)^{-1/2}, \tag{15}$$

$$\lambda = \lambda_1 b,\ \Pr = \frac{\rho_0 C_p v_0}{K_0},\ \text{and}\ \theta = \frac{T-T_0}{T_s - T_0}.$$

The associative boundary conditions are for stretching

$$f' = 1,\ f = S,\ \theta = 1\ \text{at}\ y = 0 \tag{16}$$

$$f = 0,\ f'' = 0,\ \theta' = 0\ \text{at}\ y = \beta. \tag{17}$$

3. Solution by Homotopy Analysis Method for Stretching

For homotopy analysis method (HAM) solution, we select following initial approximations and auxiliary linear operators

$$f_0(\eta) = S + \eta + \left(\frac{\eta^3}{\beta} - 3\eta^2\right)\left[\frac{S}{2\beta^2} + \frac{1}{2\beta}\right], \tag{18}$$

$$\theta_0(\eta) = \frac{1}{2}\eta^2 - \beta\eta + 1, \tag{19}$$

$$L_v(f) = \frac{\mathrm{d}^4 f}{\mathrm{d}\eta^4}(\eta),\quad L_v(\theta) = \frac{\mathrm{d}^2\theta}{\mathrm{d}\eta^2}(\eta), \tag{20}$$

and the properties satisfied by the auxiliary linear operators are

$$L_v\left[C_1 + C_2\eta + C_3\eta^2 + C_4\eta^4\right] = 0,\quad L_\theta[C_5 + C_6\eta], \tag{21}$$

in which $C_i (i = 1-6)$ are arbitrary. If $P \in [0,1]$ is an embedding parameter and $h_i (i = 1-2)$ are non-zero auxiliary parameters then the *zeroth- and mth-order deformation* problems are as follows:

i) Zeroth-order deformation problems for stretching

$$(1-p)L_v\left[\hat{f}(\eta,p) - f_0(\eta)\right] = p\hbar_v H_v N_v[\hat{f}(\eta,p)], \tag{22}$$

$$(1-p)L_\theta\left[\hat{\theta}(\eta,p) - \theta_0(\eta)\right] = p\hbar_\theta H_\theta N_\theta\left[\theta(\eta,p)\right], \tag{23}$$

$$\hat{f}'(0,p) = 1,\ \hat{f}(0,p) = S,\ \hat{f}(\beta,p) = 0,\ \hat{f}''(\beta,p) = 0, \tag{24}$$

$$\hat{\theta}(0,p) = 1, \hat{\theta}'(\beta,p) = 0, \tag{25}$$

$$N_v[\hat{f}(\eta,\xi,p)] = \hat{f}\frac{\partial^2\hat{f}}{\partial\eta^2} - \left(\frac{\partial\hat{f}}{\partial\eta}\right)^2 - \lambda\left(\hat{f}^2\frac{\partial^3\hat{f}}{\partial\eta^3} - 2f\frac{\partial\hat{f}}{\partial\eta}\frac{\partial^2\hat{f}}{\partial\eta^2}\right) - (1-A\hat{\theta})\left[A\frac{\partial\hat{\theta}}{\partial\eta}\frac{\partial^2\hat{f}}{\partial\eta^2} - \frac{\partial^3\hat{f}}{\partial\eta^3}\right], \tag{26}$$

$$N_\theta[\hat{\theta}(\eta,\xi,p)] = \Pr\left[2\frac{\partial\hat{f}}{\partial\eta}\hat{\theta} - \hat{f}\frac{\partial\hat{\theta}}{\partial\eta}\right] - (1-\delta\hat{\theta})\frac{\partial^2\hat{\theta}}{\partial\eta^2} - \delta\left(\frac{\partial\hat{\theta}}{\partial\eta}\right)^2. \tag{27}$$

ii) mth-order deformation problems for stretching

$$L_v[f_m(\eta) - \chi_m f_{m-1}(\eta)] = \hbar_v R_v(\eta), \tag{28}$$

$$L_\theta[\theta_m(\eta) - \chi_m\theta_{m-1}(\eta)] = \hbar_\theta R_\theta(\eta), \tag{29}$$

$$\hat{f}_m'(0) = 1,\ \hat{f}_m(0) = S,\ \hat{f}_m(\beta) = 0,\ \hat{f}_m''(\beta) = 0, \tag{30}$$

$$\theta_m(0) = 1,\ \theta_m'(\beta) = 0. \tag{31}$$

$$R_v(\eta) = \sum_{k=0}^{m-1}\left[f_{m-1-k}\frac{\partial^2 f_k}{\partial\eta^2} - \frac{\partial f_{m-1-k}}{\partial\eta}\frac{\partial f_k}{\partial\eta}\right] - \lambda\left[\sum_{k=0}^{m-1} f_{m-1-k}\left(\sum_{l=0}^{k} f_{k-l}\frac{\partial^3 f_l}{\partial\eta^3}\right)\right] + \lambda\left[\sum_{k=0}^{m-1} f_{m-1-k}\cdot\left(\sum_{l=0}^{k}\frac{\partial f_l}{\partial\eta}\frac{\partial^2 f_l}{\partial\eta^2}\right)\right]\left[A\sum_{k=0}^{m-1}\frac{\partial\theta_{m-1-k}}{\partial\eta}\frac{\partial^2 f_k}{\partial\eta^2} - \frac{\partial^3 f_{m-1}}{\partial\eta^3}\right] - \left[A^2\sum_{k=0}^{m-1}\theta_{m-1-k}\left(\sum_{l=0}^{k}\frac{\partial\theta_{k-l}}{\partial\eta}\frac{\partial^2 f_k}{\partial\eta^2}\right) - \sum_{k=0}^{m-1}\theta_k\frac{\partial^3 f_{m-1-k}}{\partial\eta^3}\right], \tag{32}$$

$$R_\theta(\eta) = \Pr\left[2\sum_{k=0}^{m-1}\theta_{m-1-k}\frac{\partial f_k}{\partial\eta} - \sum_{k=0}^{m-1}\frac{\partial\theta_{m-1-k}}{\partial\eta}f_k\right] - \frac{\partial^2\theta_{m-1}}{\partial\eta^2} + \delta\left[\sum_{k=0}^{m-1}\theta_{m-1-k}\frac{\partial^2\theta_k}{\partial\eta^2} + \sum_{k=0}^{m-1}\frac{\partial\theta_{m-1-k}}{\partial\eta}\frac{\partial\theta_k}{\partial\eta}\right], \tag{33}$$

$$\chi_m = \begin{cases} 0, & m \le 1, \\ 1, & m > 1. \end{cases} \tag{34}$$

The symbolic software Mathematica is used to get the solutions of (28) and (29) up to the first few orders of approximation. It finds that the solution for f and θ are

$$f(\eta) = \sum_{m=0}^{\infty} f_m(\eta) = \sum_{n=0}^{7m+3} a_{m,n}\eta^n, \tag{35}$$

$$\theta(\eta) = \sum_{m=0}^{\infty} \theta_m(\eta) = \sum_{n=0}^{7m+1} b_{m,n}\eta^n, \tag{36}$$

in which the coefficients $a^q_{m,n}$ and $b^q_{m,n}$ of $f_m(\eta)$ and $\theta_m(\eta)$ can be determined by using the given boundary conditions and by initial guess approximations in (18) and (19). The numerical data of the above mentioned solutions have been presented through graphs.

3.1. Shrinking Sheet Problem

For shrinking phenomena, the governing equations are (13) and (14), however, the boundary conditions for shrinking case are as follows:

$$\hat{f}'(0) = -1, \ \hat{f}(0) = S, \ \hat{f}(\beta) = 0, \ \hat{f}''(\beta) = 0, \tag{37}$$

$$\hat{\theta}(0) = 1, \ \hat{\theta}'(\beta) = 0. \tag{38}$$

The solution of the above boundary value problem has been calculated using the procedure discussed in the previous section of stretching. To avoid the repetition, the complete solution is not defined here but some necessary things are as follows:

$$f_0(\eta) = S - \eta + \left(\frac{\eta^3}{\beta} - 3\eta^2\right)\left[\frac{S}{2\beta^2} - \frac{1}{2\beta}\right], \tag{39}$$

$$\theta_0(\eta) = \frac{1}{2}\eta^2 - \beta\eta + 1. \tag{40}$$

4. Results and Discussion

The analytic solutions of the problem defined by (13) and (14) have been computed by HAM. The solutions (35) and (36) contain non-zero auxiliary parameters $\hbar_i$ $(i = 1-2)$ which can adjust and control the convergence of the solutions. The $\hbar$-curve are displayed to ensure the convergence of the solutions in the admissible range of the values of the auxiliary parameters $\hbar_i$. In the present cases, the 20th and 16th order of $\hbar_i$-curves are plotted in Figures 1–4. It is seen from these figures that the ranges for the admissible values of $\hbar_i$ are $0 \le \hbar_1 \le 3.5$ and $0.6 \le \hbar_2 \le 1.5$ for both stretching and shrinking phenomena.

4.1. Graphical Behaviour of the Physical Parameters

The velocity field f' and the temperature field θ are plotted in Figures 6–25 for some values of parameter A (variable viscosity), δ (thermal conductivity parameter), β (height of fluid film), S (suction velocity), and Pr (Prandtl number). The nondimensional velocity f' is plotted against η for different values of β both for stretching and shrinking phenomena (see Figs. 6–7). It is seen that with the increase in β the velocity field decreases for the stretching case and increases for the shrinking case. The variation of β on temperature profile is shown in Figures 8–9. It is observed from these figures that with the increase in β the temperature profile decreases for the stretching case and increases for the shrinking case. The velocity field f' for different values of λ is plotted in Figures 10–11. It is observed that with the increase in λ in the stretching case f' decreases near the plate but away from the plate the re-

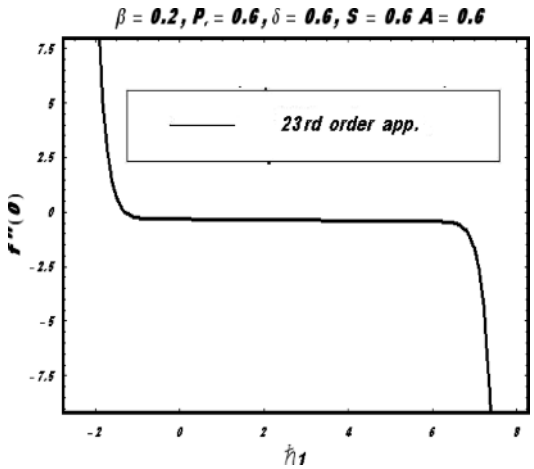

Fig. 2. $\hbar$ curve for the velocity field for stretching.

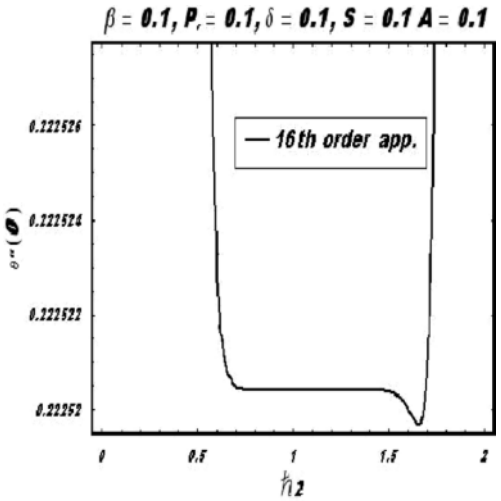

Fig. 3. $\hbar$ curve for the temperature field for stretching.

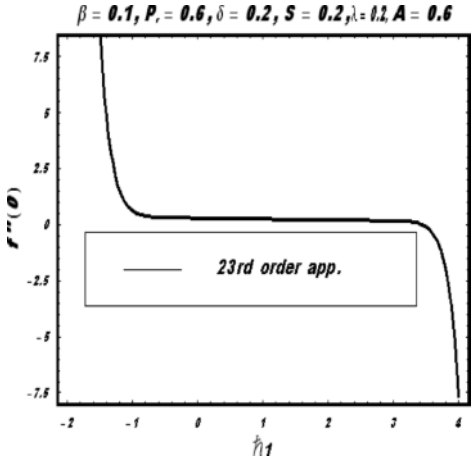

Fig. 4. $\hbar$ curve for the velocity field for shrinking.

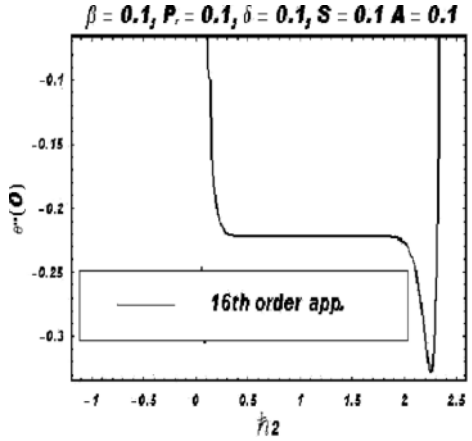

Fig. 5. $\hbar$ curve for the temperature field for shrinking.

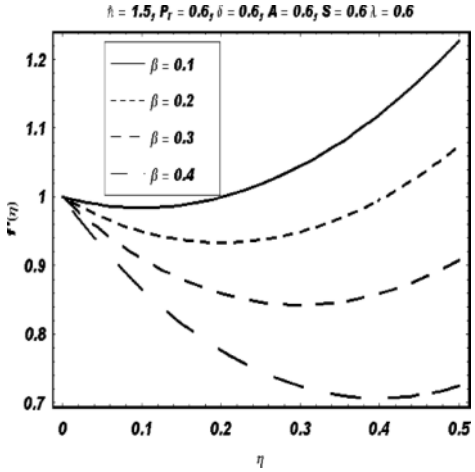

Fig. 6. Velocity field for different values of β for the stretching case.

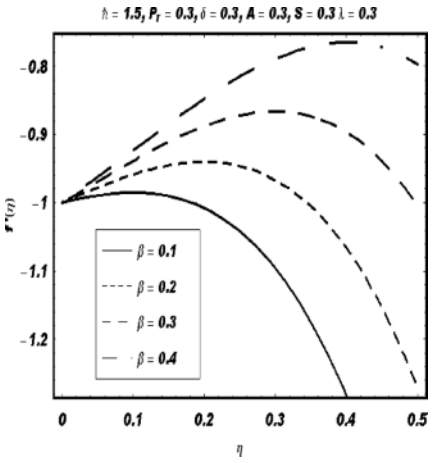

Fig. 7. Velocity field for different values of β for the shrinking case.

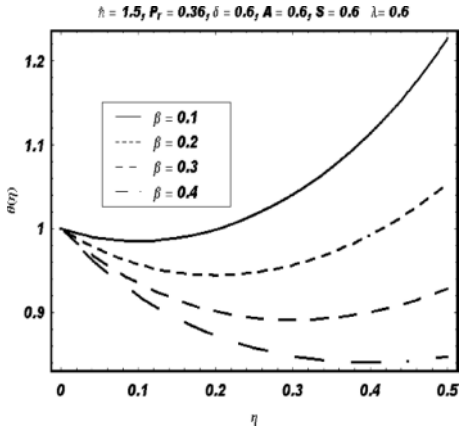

Fig. 8. Temperature field for different values of β for the stretching case.

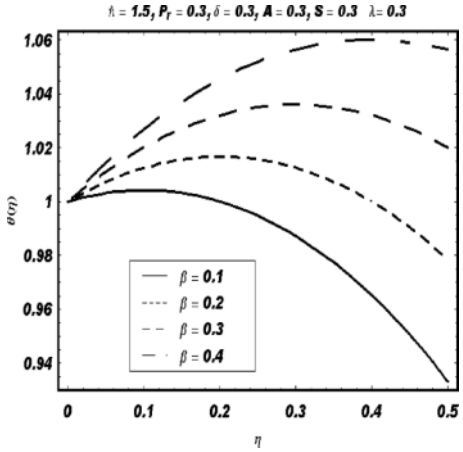

Fig. 9. Temperature field for different values of β for the shrinking case.

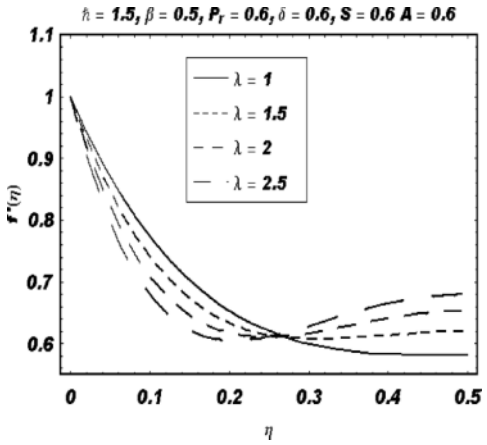

Fig. 10. Velocity field for different values of λ for the stretching case.

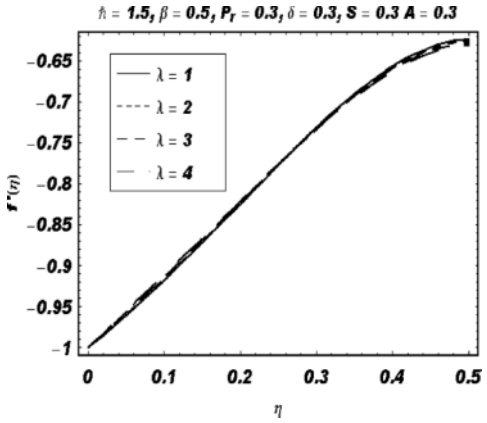

Fig. 11. Velocity field for different values of λ for the shrinking case.

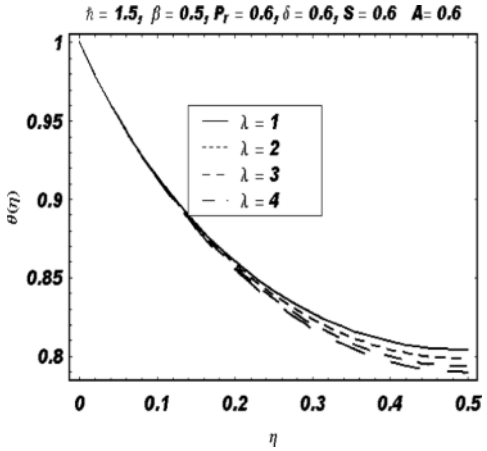

Fig. 12. Temperature field for different values of λ for the stretching case.

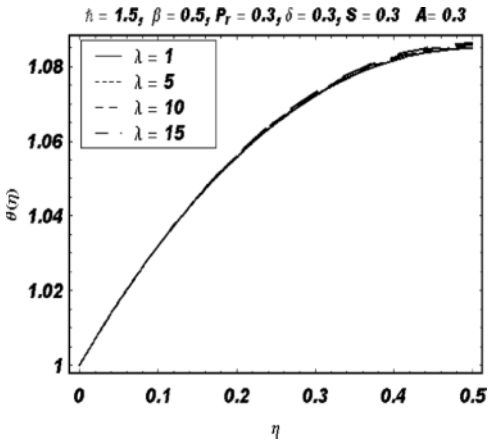

Fig. 13. Temperature field for different values of λ for the shrinking case.

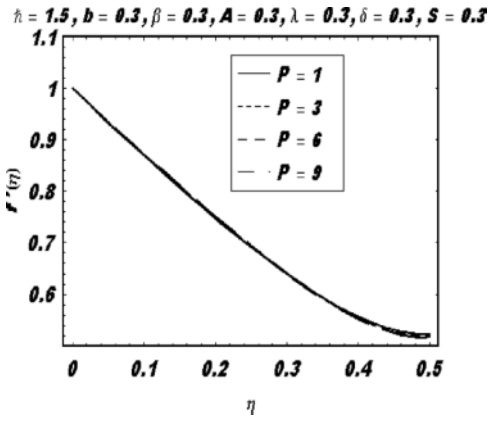

Fig. 14. Velocity field for different values of P for the stretching case.

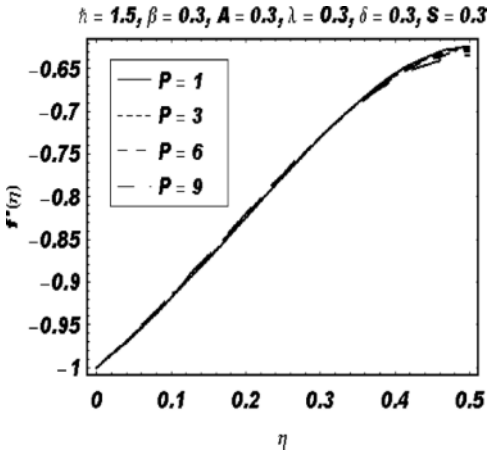

Fig. 15. Velocity field for different values of P for the shrinking case.

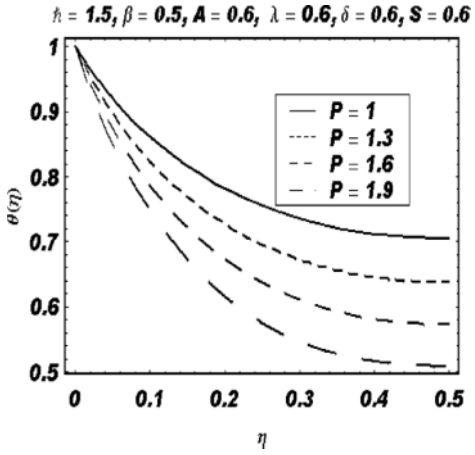

Fig. 16. Temperature field for the different values of P for the stretching case.

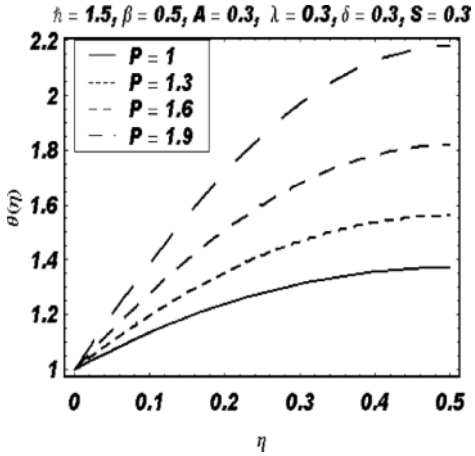

Fig. 17. Temperature field for the different values of P for the shrinking case.

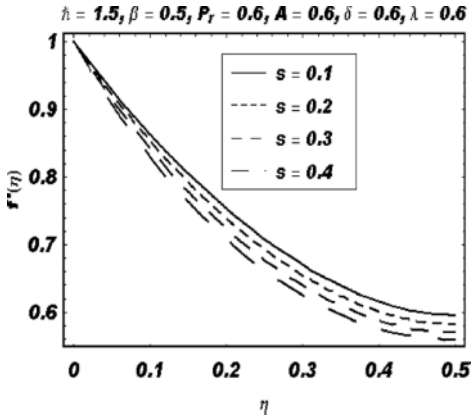

Fig. 18. Velocity field for the different values of S for the stretching case.

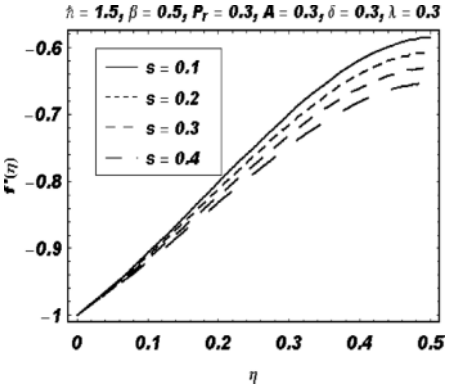

Fig. 19. Velocity field for the different values of S for the shrinking case.

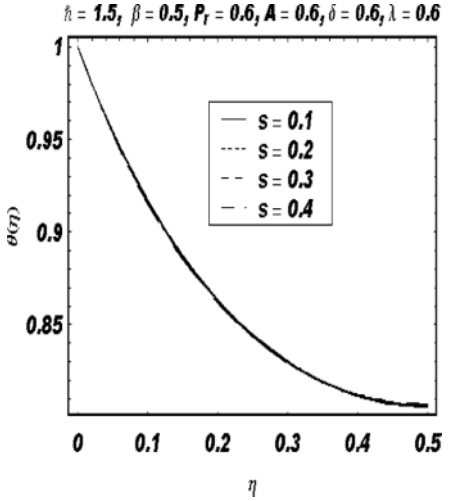

Fig. 20. Temperature field for the different values of S for the stretching case.

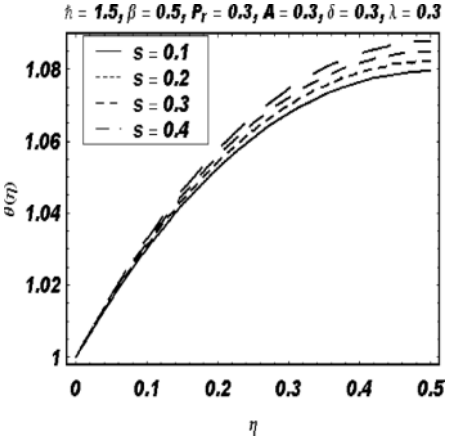

Fig. 21. Temperature field for the different values of S for the shrinking case.

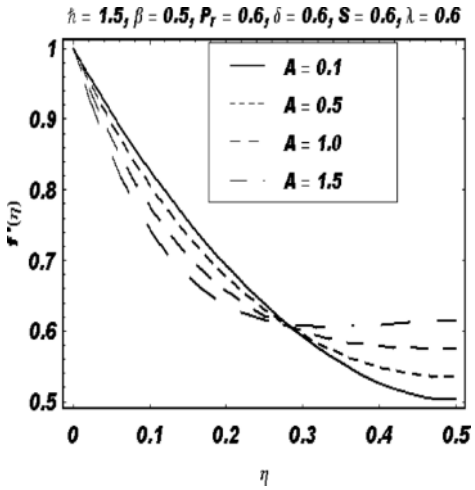

Fig. 22. Velocity field for the different values of A for the stretching case.

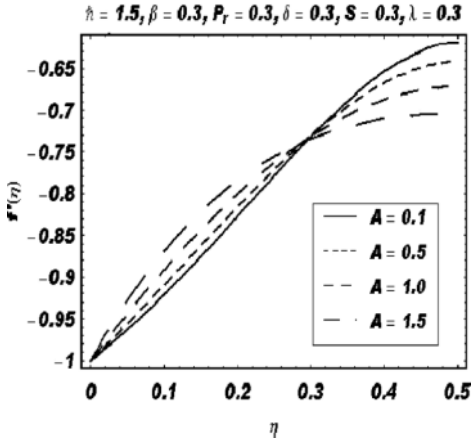

Fig. 23. Velocity field for the different values of A for the shrinking case.

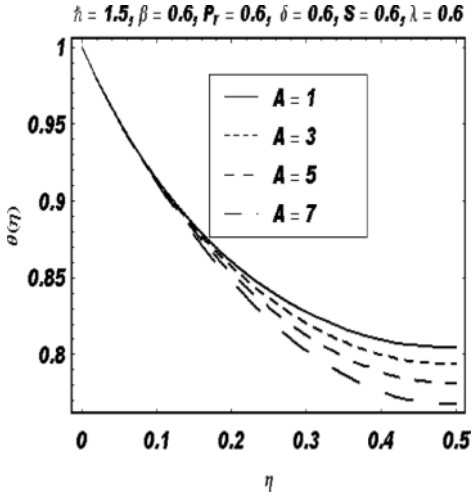

Fig. 24. Temperature field for the different values of A for the stretching case.

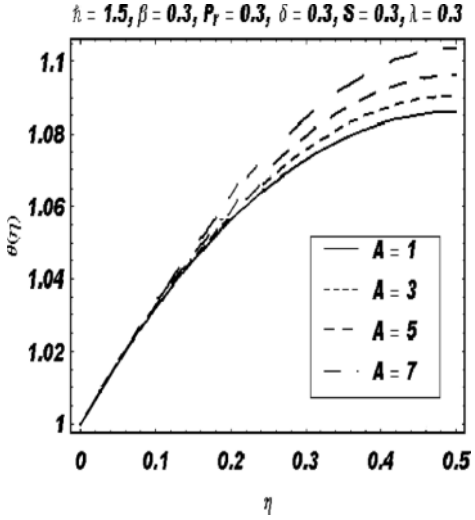

Fig. 25. Temperature field for the different values of A for the shrinking case.

sults are quite opposite, however, for the shrinking case the variation is not very prominent but the behaviour of the velocity is reversed as compared to stretching. Figures 12 – 13 are prepared for temperature field variation with λ. It is depicted that the temperature field decreases with the increase in λ for the stretching case while increases with the increase in λ for the shrinking case. There is very slight variation in velocity with the variation of the Prandtl number Pr (see Figs. 14 – 15). The temperature profile is showing very prominent results with the variation of the Prandtl number Pr, which are shown in Figures 16 – 17. It is observed that with the increase of Pr, θ decreases in the stretching case and increases in the shrinking case. The variation of S on the velocity field is almost similar as discussed for the case of variation of β (see Figs. 18 – 19). The effect of S on the temperature profile is almost negligible which is shown in Figures 20 – 21. The velocity field f' for different values of A is shown in Figures 22 – 25. It is observed that these results are almost similar as we have already discussed for the case of variation of λ. The temperature profile decreases with the increase of A for stretching while the results are quite opposite for the shrinking phenomena.

5. Conclusion

The visco–elastic fluid flow equations in the presence of temperature dependent viscosity over a shrinking/stretching sheet are derived in this paper. The nonlinear problem of velocity is solved by HAM. Using this velocity, the energy equation is also solved analytically. The variations of various emerging parameters such as β, λ, P, S, and A on the velocity and temperature are discussed through graphs. The convergence of the results is shown in Figures 1–4. The main results of the present analysis are as follows:

- The effects of S and β are same on the velocity field.
- The influence of A and λ is identical on the velocity field.
- The behaviour of all parameters is quite opposite for the two cases named shrinking and stretching.

[1] T. Hayat, N. Alvi, and N. Ali, Nonlin. Anal. Real World Appl. **9**, 1474 (2008).
[2] M. Khan, S. H. Ali, and C. Fetecau, H. Qi, Appl. Math. Model. **33**, 2526 (2009).
[3] V. Aliakbar, A. A. Pahlavan, and K. Sadeghy, Commun. Nonlin. Sci. **14**, 779 (2009).
[4] A. A. Pahlavan, V. Aliakbar, F. V. Farahani, and K. Sadeghy, Commun. Nonlin. Sci. **14**, 473 (2009).
[5] M. Ghoreishi, A. I. B. M. Ismail, A. K. Alomari, and A. Sami Bataineh, Commun. Nonlin. Sci. **17**, 1163 (2012).
[6] M. Ghoreishi, A. I. B. M. Ismail, and A. K. Alomari, Math. Comput. Model. **54**, 3007 (2011).
[7] Y. J. Jian, Q. S. Liu, and L. G. Yang, J. Non-Newtonian Fluid Mech. **166**, 1304 (2011).
[8] Q. S. Liu, Y. J. Jian, and L. G. Yang, J. Non-Newtonian Fluid Mech. **166**, 9 (2011).
[9] S. Wang and W. Tan, Int. J. Heat Fluid Flow **32**, 88 (2011).
[10] L. Zheng, C. Li, X. Zhang, and Y. Gao, Comput. Math. Appl. **62**, 1105 (2011).
[11] W. Akhtar, I. Siddique, and A. Sohail, Commun. Nonlin. Sci. **16**, 2788 (2011).
[12] M. Jamil, A. Rauf, A. A. Zafar, and N. A. Khan, Comput. Math. Appl. **62**, 1013 (2011).
[13] K. R. Rajagopal, Int. J. Nonlin. Mech. **47**, 72 (2012).
[14] D. Tripathi, Comput. Math. Appl. **62**, 1116 (2011).
[15] T. Laadj and M. Renardy, Nonlin. Anal. Theor. Meth. Appl. **74**, 3614 (2011).
[16] N. Faraz, Comput. Math. Appl. **61**, 1991 (2011).
[17] Y. Khan and Q. Wu, Comput. Math. Appl. **61**, 1963 (2011).
[18] Z. Zhang, Turk. J. Phys. **32**, 235 (2008).
[19] Z. Zhang, Z. Liu, X. Miao, and Y. Chen, Appl. Math. Comput. **216**, 3064 (2010).
[20] Z. Zhang, Y. Li, Z. Liu, and X. Miao, Commun. Nonlin. Sci. **16**, 3097 (2011).
[21] Z. Zhang, Z. Liu, X. Miao, and Y. Chen, Phy. Lett. A **375**, 1275 (2011).
[22] X. Miao and Z. Zhang, Commun. Nonlin. Sci. **16**, 4259 (2011).
[23] Z. Zhang and X. Gan, D. Yu, Z. Naturforsch. **66a**, 721 (2011).
[24] S. J. Liao, The Proposed Homotopy Analysis Technique for the Solution of Nonlinear Problems, Ph. D. thesis, Shanghai Jiao Tong University 1992.
[25] S. J. Liao, Appl. Math. Comput. **147**, 499 (2004).
[26] Y. J. Li, B. T. Nohara, and S. J. Liao, J. Math. Phys. **51**, 063517 (2010).
[27] C. Wang and I. Pop, Int. J. Non-Newtonian Fluid Mech. **138**, 161 (2006).
[28] I. C. Liu and H. I. Andersson, Int. J. Thermal Sci. **47**, 996 (2008).
[29] B. S. Dandapat, B. Santra, and K. Vajravelu, Int. J. Heat Mass Tran. **50**, 991 (2007).
[30] S. Nadeem and M. Awais, Phy. Lett. A **372**, 4965 (2008).
[31] S. Nadeem and N. Faraz, Chinese Phys. Lett. **27**, 034704 (2010).
[32] B. Raftari, S. T. Mohyud-Din, and A. Yıldırım, Science China Ser. G **54**, 342 (2011).
[33] A. Yıldırım and S. A. Sezer, Z. Naturforsch. **65a**, 1106 (2010).
[34] Y. Khan, Q. Wu, N. Faraz, and A. Yıldırım, Comput. Math. Appl. **61**, 3391 (2011).
[35] Y. Khan, Q. Wu, N. Faraz, A. Yıldırım, and S. T. Mohyud-Din, Z. Naturforsch. **67a**, 721 (2012).